RESEARCH ARTICLE

Fourier Transform Infrared Spectroscopy as diagnostic tools for bladder cancer treatment: Doxorubicin and Cisplatin and Reduced Graphene Oxide as nanocarrier

Fávaro, Wagner J.[1], Ceragioli, Helder J.[2], Villela Renata A.[3], Duran, Nelson[3]*

[1] *Laboratory of Urogenital Carcinogenesis and Immunotherapy, Biological Institute, Department of Structural and Functional Biology, University of Campinas, Campinas-SP, Brazil*

[2] *EEC, University of Campinas, Campinas-SP, Brazil*

[3] *Nanomed Center, Federal University of ABC, Santo André, SP., Brazil*

ARTICLE INFO

ABSTRACT

Objective(s): The use of Fourier Transform Infrared Spectroscopy (FTIR) as diagnostic tools for bladder cancer associate to histopathology analysis.

Methods: FTIR imagens of normal and bladder cancer tissues in rats o Brucker model V 70 spectrophotometer provided with the MCT detector (Mercury Cadmium Telluride), under attenuated total reflectance (ATR). Histopathology analysis of rat tissues and comparison of diagnostics in both methods.

Results: All the spectroscopic parameters analyzed showing that the progress of cancer treatment were consistent with the histopathological analyses. The ratio of FTIR bands intensity of protein/lipid (I1633/I1743) was highly increased (ratio of 3.33) in the cancer tissues compared with normal one (ratio of 1.22). After treatment with DOX-CIS-rGO nanocarrier a value of protein/lipid ratio was 1.38.

Conclusions: All data of the ATR-FTIR imagens will be important tools for the most complex and expensive histopathological analysis. The ATR-FTIR diagnosis will be an important data in the final decision related to progress in the chemotherapeutic treatment. Of course, the fast analysis by ATR-FTIR methodology compared to histopathology could be an important support for monitoring all these studies.

INTRODUCTION

Exist various methods to detect bladder cancer, however, different assays exhibit several degrees of accuracy that intrinsically depends on the quality of the method. Urine makers and cystoscopy (among others) exhibit the same sensitivity and specificity of 97.2% and 97%, respectively. But in urine markers the disadvantages are many leading to a high inter-observer variability. Cytoscopy exhibits difficulties, mainly due to selection of tumor samples and it involves instrumentation risks, urethral injury, urinary tract contamination and haematuria [1]. Besides these two important diagnostic assays, there are other that evaluate bladder cancer staging and bladder wall, such as, MRI (magnetic resonance imaging) (72%−96%) and CDE-MRI (dynamic contrast-enhanced MRI) is helpful and supply images of muscle invasion with precision around 85%. Apparent diffusion coefficient (ADC) and diffusion-weighted imaging (DWI) are adequate methods for analysis of surrounding tissue and tumor invasion. The evaluation of lung metastases in the bladder cancer diagnosis, Chest plain X-ray film or CT (computed tomography) plain scan should be programed and performed routinely, as well as bone scintigraphy, CT scan on MRI to exclude bone metastases. But, any diagnostic CT or MRI uncertains and execution of positron emission tomography-CT (PET-CT)

* Corresponding Author Email: *nduran@unicamp.br*

continue to exist [2].

A significant report on folic acid-modified mesoporous silica nanospheres, carried with gadolinium (Gd) in cancer detection (*in vitro*), showed that relaxometry analysis by MRI images, showed that this nanospheres were excellent T1-weighted contrast agents (CAs) by delivering a sufficient amount of Gd3+ as CAss into cancer cells. The authors stated that these outcomes afford useful insights for increasing approaches to design efficient CA to nanoparticles transport [3].

One of the best diagnosis is histophatology and immunohistochemistry due to the detection gives chances to estimates bladder cancer markers, but they have the disadvantage that it is a necessary a very specialized anatomists and the costs are high [2].

The Fourier Transform Infrared Spectroscopy (FTIR) imaging application to medical samples has been reported in many reports [4]. Applications centered in focusing on imaging and fiber-optical techniques were discussed on human organs, in especial prostate, bladder, lung, liver, heart and spleen. Previously, it was discussed the possibility and prospects of these techniques in biodiagnostics to detect and characterize malignant diseases, such as tumors and other pathologies [5,6]. Advances in the Attenuated Total Reflectance (ATR) FTIR spectroscopic imaging on proteins led to understand and development of protein interaction with surfaces. Some comments on cancer cells were also done [7].

Very recently a review described a protocol in order to collect FTIR spectra and emphasized on the adequate sample preparation, alternative sampling modes as an important way to acquire spectral data were discussed [8].

Related to bladder cancer using this methodology, a series of papers with very similar profile were reported. In these studies relevant spectroscopic divergences were found between normal and malignant bladder tissues, studied by FTIR, where the spectra alterations indicate alterations in the proteins, lipids and nucleic acids ratios [9-11]. But no comparison with classical histopathological diagnosis was discussed.

Pezzei et al. [12] showed a relationship between FTIR microscopic imaging and the morphological tissue characteristics in bladder carcinoma achieved by histological staining of the sections showed that many histomorphological tissue patterns can be viewed in the color images. Similar results with

ATR-FTIR spectra on rat tissue were also published [13].

Hughes et al. [14] suggested that bladder urothelial carcinomas were a heterogeneous group of tumors. In other words, this pointed out, that sample of non-tumor or tumor zone of the same bladder must be carefully analyzed in function of the possible transformation of the close tissues, although not histopathological analysis showed they were not infiltrated [15].

Severcan et al. [16] studied ATR-FTIR spectroscopy for diagnostic device for urinary bladder cancer along with chemometric analyses (e.g., cluster and principal component). This study showed important modifications in protein, lipid, and nucleic acid distribution of bladder samples between cancer groups as comfrontrd to the normal bladder samples. An extension of this report was done by Gok et al [17].. Similar study was applied to colorectal tissues [18]. Although all these data, some care must be considered due to the different parameters involved in this measurement [19].

The bands at 1454 cm^{-1} and 1400 cm^{-1} normally attribute to the C-H bending vibrations of several amino acid side chains and few lipids. The band intensity ratio of $I_{1454}/_{1400}$ was augmented in normal cells/tissues and decreased in ovarian cancer cells/tissues [20].

Then, the aim of this study was to analyze the FTIR as tool for non-muscle invasive bladder cancer (NMIBC) therapy with doxorubicin and cisplatin drugs associated to reduced graphene oxide as carrier in the bladder cancer on rats induced chemically and its monitoring of the cancer treatment as compared to histopathological analysis.

In the introduction of the manuscript it was stated the aims of this study, and for its comprehension an overview of the previous reports were also discussed, indicating the importance of this research area.

METHODS
The workflow of the experiments was the following (Scheme 1):

Synthesis of reduced graphene oxide (rGO)
rGO was synthesized and characterized as previously reported [21,22]. Briefly: The graphene oxide films were obtained from catalytic transformation, using hot-filament chemical vapor deposition (HFCVD) reactor feedstock by
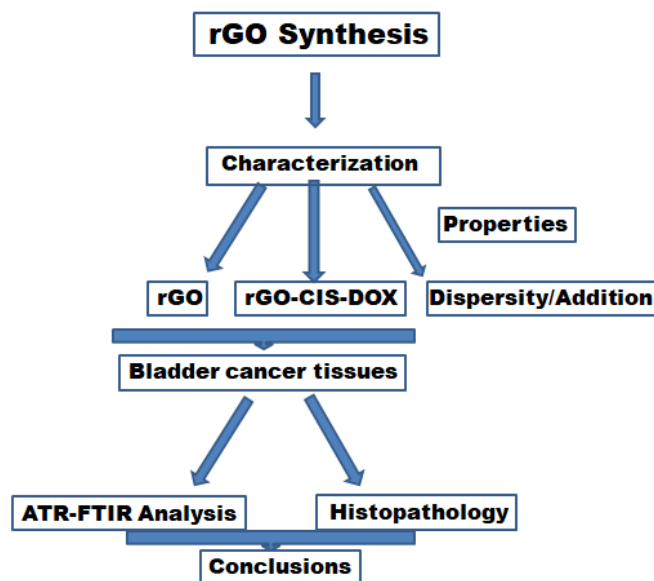
Scheme 1. Workflow of the experiments

(1:1:1) camphor/acetone/citric acid vapor solution, that were lugged by hydrogen flow. The catalytic transformation is carried under 20 Torr pressure and in 150 standard cubic centimeters per minute (sccm) of N_2 and 40 sccm of O_2 gases atmosphere. The deprivation temperature were determined at the backside of the substrate and kept constant at 450ºC along of the 30 min catalysis. The growth temperature was kept for 1 min in only hydrogen atmosphere for reducing the graphene oxide. After this, the reactor was chilled abruptly in hydrogen flux. Doxorubicin (DOX) and Cisplatin (CIS) were obtained from LC Laboratories (*Woburn, EUA*) and from Libbs Farmacêutica LTDA (*Embu, São Paulo, Brasil*), respectively. The stabity of rGO aqueous suspensio was due to electrostatic repulsion (zeta potential of −25 ± 0.18 mV) and the residual oxygen functional groups presence at defect sites. In the experiment freshly-suspended rGO was determined related to particle size, zeta potential and polydispersity index (PDI) DLS (dynamic light scattering) analysis at pH 7.6 and 25 °C; rGO exhibited an average diameter of 342 ± 23.5 nm and a PDI of 0.56 ± 0.03. These data indicate that rGO was nanosize scale with a high polydispersity.

Disperssion of rGO in Pluronic® F68

The rGO dispersion was prepared by addition of an adequate amount of rGO in 1% of Pluronic F68 in order to get a final concentration of 2 mg/ mL by ultrasonication bath by 20 min.

Adhesion of CIS and DOX on the rGO

It was added 2 mg of DOX in 1 mL of physiological solution and added 1 mL of dispersion of rGO (2 mg/mL). To 0.2 mL of CIS (0.05 mg) was added 1.0 mL of the rGO dispersion (2mg/mL) and shacked for 2 h.

In vivo experiment with rats (standard procedure in our laboratory [23]

Twenty female Fischer 344 rats 7 weeks old were purchased from the Multidisciplinary Center for Biological Investigation (CEMIB) at the University of Campinas (UNICAMP). The rat experiments were confirmed by an institutional Committee for Ethics in Animal Use (CEUA/UNICAMP, protocol no.3569-1). Previous to intravesical catheterization with a 22-gauge angiocatheter, the animals were anesthetized with 10% ketamine (60 mg/kg, i.m.; Vibra®, Roseira, SP, Brazil) and 2% xylazine (5 mg/kg, i.m.Vibra®, Roseira, SP, Brazil). The rats remained anesthetized around 45 min after catheterization to avoid spontaneous micturition. Five control animals (Control group – Group 1) received 0.30 ml of 0.9% physiological saline, intraperitoneally (i.p.), every other week (week 0, 2, 4, 6) and, after once a week for six consecutive weeks (Scheme 2). NMIBC induction was executed in 20 rats that received N-methyl-N-nitrosourea (MNU)
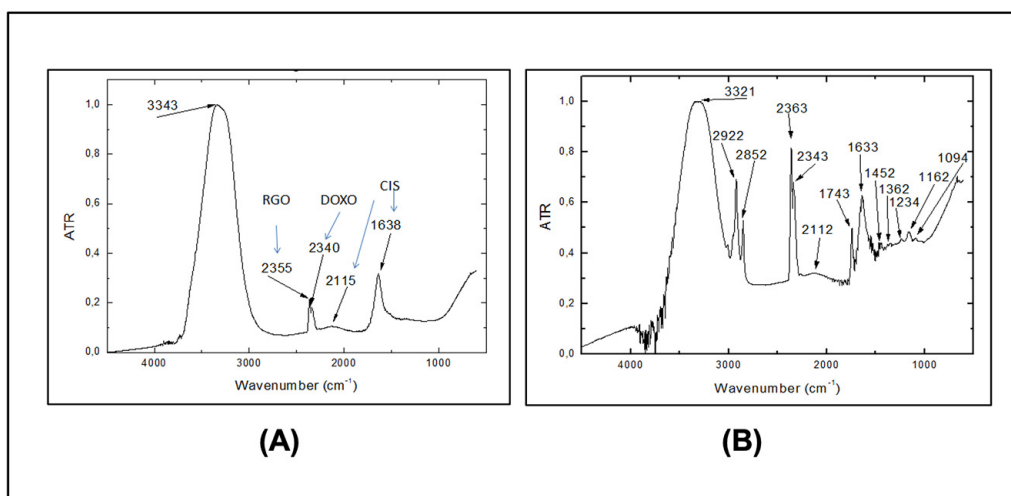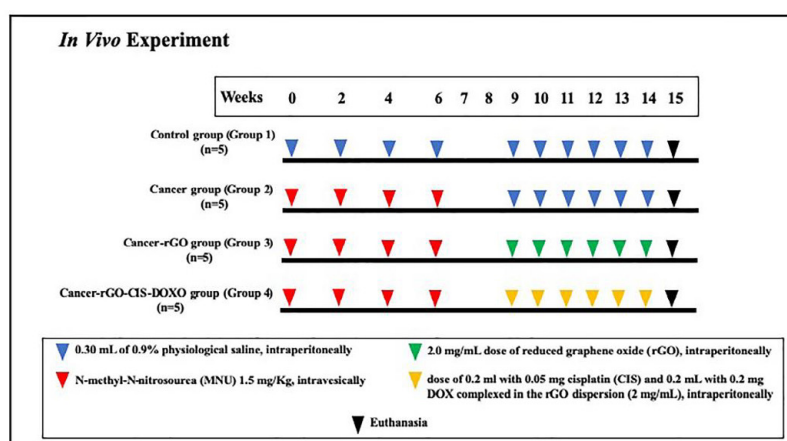
Fig. 1. (A) ATR-FTIR spectrum of the pharmaceutical (Doxorubicin-DOX, Cisplatin-CIS and reduced graphene oxide-rGO as carrier). (B) ATR-FTIR spectrum of non-cancer bladder tissue as control.

Scheme 2. Scheme of the in vivo experiments.

1.5 mg/Kg, dissolved in 0.30 ml of 1 M sodium citrate, pH 6.0, intravesically, every other week (week 0, 2, 4, 6), totaling 4 doses (Fig. 1). Two weeks after the last dose of MNU, all rats were studied by ultrasonography to evaluate the incidence of tumors. MNU-treated rats were further divided into 3 groups (n=5 per group): the Cancer group (Group 2) received 0.30 ml of 0.9% physiological saline, i.p., once a week for six consecutive weeks (Scheme 2); the Cancer-rGO group (Group 3) received 2.0 mg/mL dose of reduced graphene oxide (rGO), i.p., once a week for six consecutive weeks (Scheme 2); the Cancer - rGO - CIS - DOXO group (Group 4) received a dose of 0.2 ml with 0.05 mg cisplatin (CIS) and 0.2 mL with 0.2 mg DOX complexed in the rGO dispersion (2 mg/mL), i.p.,

once a week for six consecutive weeks (Scheme 2). After the treatment, all animals were euthanized, and the urinary bladders were surgically extracted and collected and submitted to histopathological and FTIR spectroscopy analyses.

Histopathological Analysis

Samples (small pieces) of urinary bladders from all animals that were surgically extracted and collected were fixed in Bouin solution for 12 hours. Then, after fixation, the tissues were washed in 70% ethanol, followed by dehydration in an ascending series of alcohols. Then, the fragments were diaphanized in xylene for 2 h and enclosed in plastic polymers (*Paraplast Plus, ST. Louis, MO, USA*). Then, the materials were cut on a
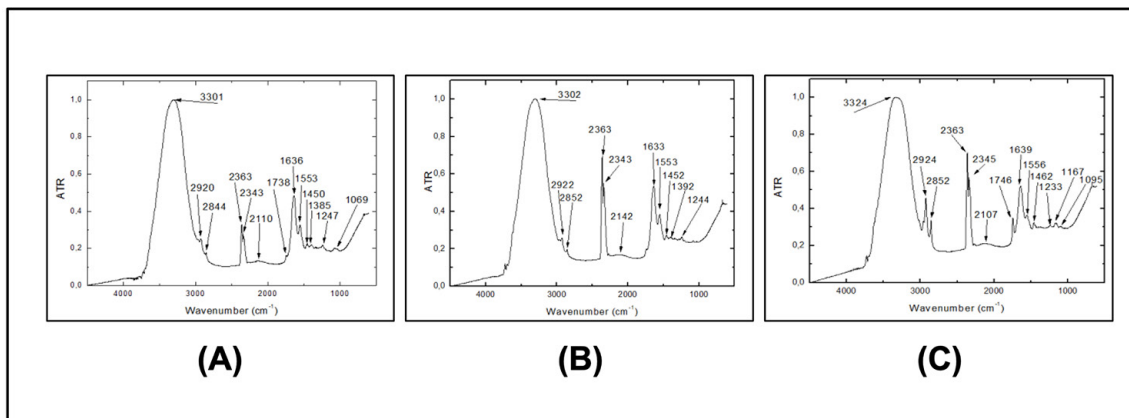
Fig. 2. (A) FTIR spectrum of cancer bladder tissue; (B) FTIR spectrum of cancer bladder after treatment with rGO as carrier; (C) FTIR spectrum of cancer bladder tissue after treatment with rGO, CIS and DOX simultaneously.

rotary microtome Leica RM 2165 (*Leica, Munich, Germany*) with a thickness of 5 μm and stained with hematoxylin-eosin and photographed in the light microscope Zeiss Axiophot (*Zeiss, Munich, Germany*). The experimental groups were classified as consensus staging proposed by the World Health Organization/International Society of Urological Pathology [23,24].

Measurements of urinary bladder with Fourier Transform Infrared (FTIR)

Fragments of the urinary bladder were frozen immediately after euthanized in liquid nitrogen and then placed in a -80°C freezer. No chemical was used for the store the samples. All the measurements were done in fresh samples (triplicated). The model Brucker model V 70 spectrophotometer equipped with the MCT detector (Mercury Cadmium Telluride), under attenuated total reflectance (ATR) operating at liquid nitrogen temperature and connected to a spectrometer (Spectrum 400 - Perkin-Elmer). The images were collected in the range of 4000-900 cm^{-1} with 64 scans per pixel (pixel size 6.25 μm^2) and resolution of 4 cm^{-1}. After the FTIR measurements, the files were analyzed using Cytospec® software (version 1.4.02) to study the spectral matrix, which generated the infrared image. Small amounts of fresh bladder samples of tissues were pressed under vacuum and the spectra were obtained from L-neon laser with wavelength at 630 nm.

Statistical Analyses

The proportion test was used to evaluate the histopathological results. A type-I error of 5% was statistically significant for all analysis performed.

RESULTS AND DISCUSSION

Characterization of rGO and rGo-CIS-DOX derivatives

Synthesis of rGO and its properties.

Synthesis of rGO was obtained as reported by Durán et at.[21] [19] and Zanin et al.[22] [20], and dispersion in Pluronic F68 and the addition of CS and DOX in rGO [19] were also reported..

ATR-FTIR Analysis

Urinary bladder samples with cancer or normal one were maintained after frozen in a liquid nitrogen and

kept in a -80°C freezer. Small amounts of samples of tissues were pressed under vacuum and the spectra

were obtained from L-neon laser with wavelength at 630 nm. **Figs. 1** and **2** illustrate the results of the analysis of tissue samples from normal and cancer samples.

Spectra measured for the DOXO-CIS-rGO as control (**Fig.1A**) and normal tissues (from normal rat) (**Fig.1B**) were assigned to proteins around 1650 cm^{-1} and 1240 cm^{-1} and lipids around 2930-2850 cm^{-1} and 1740 cm^{-1} [25]. The asymmetric and symmetric bands at 1236 cm^{-1} and 1080 cm^{-1} are due to phosphate stretching mode and from nucleic acids, respectively [26]. The C-OH stretching vibrations collagen (carbohydrates) CH$_2$ wagging and C-N stretching vibrations of collagen side chain appeared at 1200 cm^{-1} and 1030 cm^{-1} [27,28]. Besides lipids, proteins and nucleic acids,

Table 1. Ratios of FTIR Intensities of Protein, protein/Lipid, Lipid and Phosphate/Nucleic Acid Bands intensities.

SAMPLES	Protein ratio I_{1633}/I_{1553}	Protein/Lipid ratio I_{1633}/I_{1743}	Lipid ratio I_{2922}/I_{2850}	Phosphate/ Nucleic acid $I_{1094}I_{1234}$
Control	1,390 ± 0.062	1.220 ± 0.054	1.340 ± 0.030	1.050 ± 0.042
Bladder cancer	1.560 ± 0.069	3.330 ± 0.147	1.220 ± 0.012	1.120 ± 0.045
Bladder cancer rGO	1.480 ± 0.066	2.750 ± 0.122	1.310 ± 0.058	0.980 ± 0.039
Bladder cancer rGO-CIS-DOX	1.380 ± 0,059	1.380 ± 0.061	1.360 ± 0.060	1.010 ± 0.040

Note: Control and bladder cancer animals were different. Values are average values of 10 tissues samples from rats.rGO: reduced graphene oxide; CI'S: Cisplatin; DOX: Doxorubicin

carbohydrates appeared at around 1000-1200 cm^{-1} region [29-31][27-29]. The peaks at 1080 cm^{-1} and 1236 cm^{-1} were signaling to phosphate moiety (e.g. nucleic acids), and the bands at 2925 cm^{-1} and 2850 cm^{-1} were CH_2, CH_3 stretching vibrations of phospholipids [25].

In the Fig. 2 is shown the FTIR of cancer bladder tissue without any treatment, only with rGO

treatment and the effect of the application of CIS and DOX in the rGO as carrier.

The ratio between amide I and amide II (I_{1650}/I_{1550}) bands intensities was increased in the cancer bladder tissues (ratio of 1.56) compared to the control one (ratio of 1.39) **(Table 1).** The protein ratio increase in the cancer tissues indicated that carbonyl bonds (proteins) and hydrogen bonds in the C–hydroxyl groups of amino acids were modified after cells suffered cancer. These kinds of data were previously reported by Venkatachalam et al. [28] and Al-Muslet et al. [10].

An important aspect in our research with bladder cancer is that the effect, although low, but significant with the treatment In case of the absence of any treatment the protein ratio I_{1633}/I_{1553} was 1.56. In the case of treatment with rGO a ratio of I_{1633}/I_{1553} of 1.48, near to the normal ratio of I_{1633}/I_{1553} (1.39) was achieved. But in the treatment of bladder cancer with all the anticancer selected such as rGO-CIS-DOXO was obtained a protein ratio of 1.38. The regression to the actual normal value was an important result. **(Table 1).** This is an indication that following these parameters it is possible to see the recovering of the bladder cancer in the rats after treatment with these nanomaterials.

The ratio of protein/lipid (I_{1633}/I_{1743}) was highly increased (ratio of 3.33) in the cancer tissues compared with normal one (ratio of 1.22) **(Table 1)**. The band 1743 cm^{-1} corresponding to C=O stretching mode of lipids [29] and the 1633 cm^{-1} to amide I band. Again, the treatment with rGO

as carrier reaches a significant lower value of after cancer treatment (ratio of 2.75). However, in the case of using all the anticancer drugs (rGO-CIS-DOX the value reach almost the normal value (ratio of 1.38).

The intensity ratio of lipids I_{2922}/I_{2850} represented the total lipids in the tissues. In our study, this ratio was diminished in the cancer tissues (ratio of 1.22), compared with the normal tissues (ratio of 1.34). It is known when a decrease of relative number of methyl groups in the cancer tissues is reflected as a decrease of the intensity, or extinction of the lipid bands, and this indicating a hypomethylation that is common in cancer. This observation was also reported by Li et al. [25] and from Al- Muslet et al. [10].

The important aspects in our paper, is that this ratio (I_{2922}/I_{2850}) is a significant parameter to follow the cancer treatment. In this case for this ratio in the application of rGO treatment an increase of the ratio was also observed (ratio of 1.31) and in the case of all the drugs used simultaneously a value of 1.36 was reached.

The intensities band ratio at 1234 cm^{-1} and 1094 cm^{-1} that represents nucleic acids and phosphate modifications in the tissues were important in the malignancies diagnostics. Although, careful must be considered in this ratio since the values are too low for quantitative measurement. However, considering this limitation, the ratio of I_{1094}/I_{1234} in our research this ratio was increased in the cancer tissues (ratio of 1.12) compared with normal tissue (ratio of 1.05) reflecting a high activity of the cancer cells. Some authors suggested that a high concentration of phospholipids in tumors probably is due to the phospholipids transformation and composition modifications. Structure and stability of the membranes in these conditions probably resulting in erroneous membrane function. This was a good indication that nucleic acids and
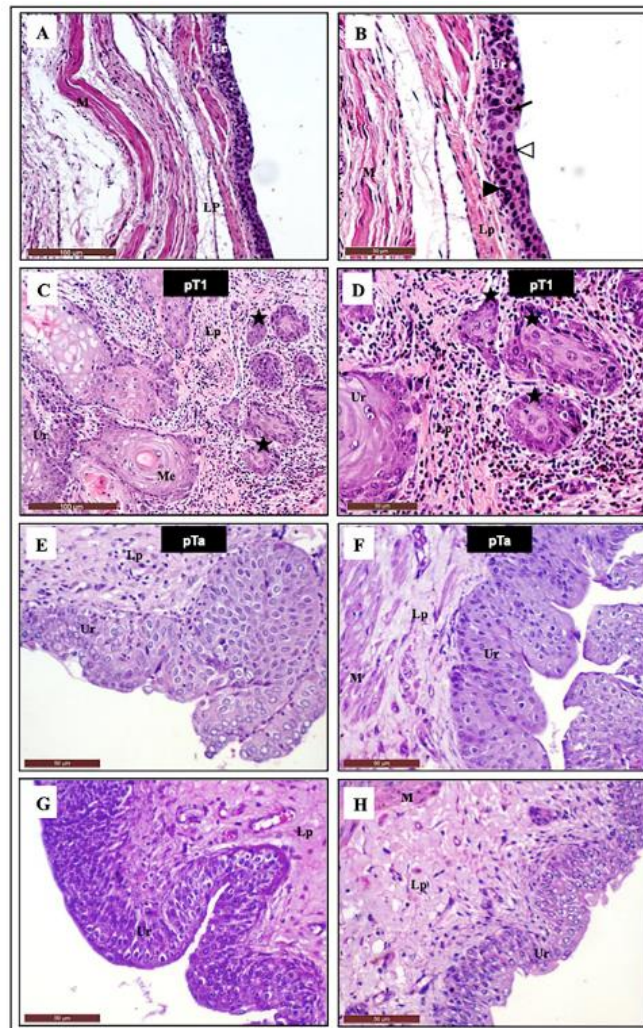
Fig. 3. Representative photomicrographs of urinary bladder from Control (a, b), Cancer (c, d), Cancer - rGO (e, f), Cancer - rGO - CIS - DOX (g, h) groups. (a), (b) Three different cell types composed the normal bladder urothelium: basal cell layer (arrowhead), intermediate cell layer (arrow) and surface cell layer (or umbrella cells, open arrowhead). (c), (d) pT1 tumor: cancer cells (stars) invading the lamina propria. (e), (f) pTa tumor: cancer cells show slender papillae with frequent branching, minimal fusion, and variations in nuclear polarity, size, shape, and chromatin pattern and with the presence of nucleoli. (g), (h) Flat hyperplasia characterized by thickening of the urothelium without cellular atypia. a – h: Lp – lamina propria, M – muscle layer, Me – Squamous metaplasia, Ur – urothelium.The most frequent neoplastic lesions in the Cancer-rGO group (Group 3) were pTa (Figures 3e, 3f), pT1 and flat carcinoma *in situ* (pTis) in 60%, 20% and 20% of the animals, respectively (Table 2).

phospholipids ratios were higher in the malignant tissues than in normal tissues. These results were in within the fate that those of Du et al.[32]. This parameter follows the same profile that the other parameters in the cancer treatment. The bladder of cancer rats for treatment with rGO alone and rGO associated to CIS and DOXO gave rate values of 0.98 and 1.01, respectively. Then, the treatment showed an important effect of cancer bladder, although low values in rats giving a near a normal values (ratio of 1.05).

On bases of these data, probably in bladder cancer the FTIR, as diagnostic, appears a simple an efficient method for following cancer treatment in rats. In order to check this statement, it was carried out the histopathological analysis in all of these treatments.

Histopathological Analysis

The Control group (Group 1) showed no histological transformations in bladder tissue (**Figs. 3a, 3b; Table 2**). Normal bladder urothelium

Table 2. Histopathological alterations (%) in urinary bladder in rats from different experimental groups

	GROUPS			
Histopathology	Group 1 (n=5)	Group 2 (n=5)	Group 3 (n=5)	Group 4 (n=5)
Normal	5 (100%)	-	-	-
Flat hyperplasia	-	-	-	02 (40%)
Low-grade Intraurothelial neoplasia	-	-	-	01 (20%)*
Flat Carcinoma *in situ* (pTis)	-	-	01 (20%)	01 (20%)*
Urothelial papillary Carcinoma (pTa)	-	01 (20%)	03 (60%)	01 (20%)
Urothelial Carcinoma with invasion of lamina própria (pT1)	-	04 (80%)	01 (20%)	-

Groups: Control (Group 1), Cancer (Group 2), Cancer-rGO (Group 3) and Cancer-rGO-CIS-DOX (Group 4). Benign lesions: Flat hyperplasia, Low-grade intraurothelial neoplasia; Malignan lesions: pTis, Pta and pT1. * $P<0.0001$ (proportions test)

composed by basal cell layer, intermediate cell layer and surface cell layer (umbrella cells) (**Figs. 3a, 3b**). In contrast, all animals from Cancer group (Group 2) showed 100% of malignant lesions, such as urothelial carcinoma with invasion of lamina propria (pT1) (**Figs. 3c, 3d**) and urothelial papillary carcinoma (pTa) in 80% and 20% of the rats, respectively (**Table 2**). Squamous metaplasia was associated with pT1 **Figs. 3c, 3d**).

Animals treated with rGO-CIS-DOX group (Group 4) neatly showed better histopathological recovery from the cancer state than those found in the other treatments, showing decrease of bladder neoplastic lesions progression in 60% of the rats (**Table 2**). Benign lesions, such as flat hyperplasia (**Figs. 3g, 3h**), were found in 40% of the animals (**Table 2**). Preneoplastic lesions such as low-grade intraurothelial neoplasia were observed in 20% of the animals. The most frequent neoplastic lesions observed in this group were pTis (20%) and pTa (20%) of the animals (**Table 2**).

All of these results with histopathology are in agreement with our observation by FTIR spectroscopy and different stages and different treatment of NMIBC cases.

Final remarks

Following the FTIR diagnostic showed that all the parameters analyzing the progress of cancer treatment are consistent with the histopathological analyses.

However, the most complex and expensive histopathological analysis is most important in the final decision related to progress in the chemotherapeutic treatment, but, as first and fast analysis the FTIR methodology could be an important support for all these studies. When is compared this methodology for detection stages in bladder cancer with other methods, such as biomarker, cystoscopy, MRI, X-rays, tomography and PET-CT, the ATR-FTIR appears as a rapid, non-expensive analysis and in agreement with the best diagnostic methods, such as histopathology analysis.

FUNDING

No funding was received.

CONFLICTS OF INTEREST/COMPETING INTERESTS

The authors declare no competing interests.

AUTHORS' CONTRIBUTIONS

All authors contributed to the study conception and design and to the experiments.

CONSENT FOR PUBLICATION

Not applicable

REFERENCE

1. Zhu C-Z, Ting H-N, Ng K-H, Ong T-A. A review on the accuracy of bladder cancer detection methods. J Cancer. 2019;10(17):4038-44.
2. Bochenek K, Aebisher D, Międzybrodzka A, Cieślar G, Kawczyk-Krupka A. Methods for bladder cancer diagnosis

– The role of autofluorescence and photodynamic diagnosis. Photodiagnosis and Photodynamic Therapy. 2019;27:141-8.

3. Hosseinabadi SZ, Safari S, Mirzaei M, Mohammadi E, Amini SM, Mehravi B. Folic acid decorated mesoporous silica nanospheres loaded with gadolinium for breast cancer cell imaging. Advances in Natural Sciences: Nanoscience and Nanotechnology. 2020;11(4):045010.

4. Kazarian SG, Chan KLA. Applications of ATR-FTIR spectroscopic imaging to biomedical samples. Biochimica et Biophysica Acta (BBA) - Biomembranes. 2006;1758(7):858-67.

5. Krafft C, Sergo V. Biomedical applications of Raman and infrared spectroscopy to diagnose tissues. Spectroscopy. 2006;20(5-6):195-218.

6. Ollesch J, Heinze M, Heise HM, Behrens T, Brüning T, Gerwert K. It's in your blood: spectral biomarker candidates for urinary bladder cancer from automated FTIR spectroscopy. Journal of Biophotonics. 2014;7(3-4):210-21.

7. Glassford SE, Byrne B, Kazarian SG. Recent applications of ATR FTIR spectroscopy and imaging to proteins. Biochimica et Biophysica Acta (BBA) - Proteins and Proteomics. 2013;1834(12):2849-58.

8. Baker MJ, Trevisan J, Bassan P, Bhargava R, Butler HJ, Dorling KM, et al. Using Fourier transform IR spectroscopy to analyze biological materials. Nat Protoc. 2014;9(8):1771-91.

9. G. Ahmed E, A. Al-Muslet N, M. Ahmed M, Moharam MA, Musaad W. The Use of Fourier Infrared Spectroscopy and Laser – Raman Spectroscopy in Bladder Malignancy Diagnosis, A comparative Study. Applied Physics Research. 2010;2(1).

10. Al-Muslet NA, Ali EE. *In vivo* spectral analysis of bladder cancer using Fourier Transform Infrared Spectroscopy, a comparative study. Australian Journal of Basic and Applied Sciences. 2011; 5(9): 1734-39.

11. Al-Muslet NA, Ali EE. Spectroscopic analysis of bladder cancer tissues using Fourier transform infrared spectroscopy. Journal of Applied Spectroscopy. 2012;79(1):139-42.

12. Pezzei C, Brunner A, Bonn GK, Huck CW. Fourier transform infrared imaging analysis in discrimination studies of bladder cancer. The Analyst. 2013;138(19):5719.

13. Staniszewska E, Malek K, Baranska M. Rapid approach to analyze biochemical variation in rat organs by ATR FTIR spectroscopy. Spectrochimica Acta Part A: Molecular and Biomolecular Spectroscopy. 2014;118:981-6.

14. Hughes C, Iqbal-Wahid J, Brown M, Shanks JH, Eustace A, Denley H, et al. FTIR microspectroscopy of selected rare diverse sub-variants of carcinoma of the urinary bladder. Journal of Biophotonics. 2012;6(1):73-87.

15. Liakou CI, Narayanan S, Tang DN, Logothetis CJ, Sharma P. Focus on TILs: Prognostic significance of tumor infiltrating lymphocytes in human bladder cancer. Cancer Immunology Research. 2007; 7(1): 1-10.

16. Severcan F, Simsek Ozek N, Gok S. Fourier Transform Infrared Spectroscopy and Imaging in Cancer Diagnosis and Characterization. Biophysical Journal. 2015;108(2):479a-80a.

17. Gok S, Aydin OZ, Sural YS, Zorlu F, Bayol U, Severcan F. Bladder cancer diagnosis from bladder wash by Fourier transform infrared spectroscopy as a novel test for tumor recurrence. Journal of Biophotonics. 2016;9(9):967-75.

18. Piva JAdAC, Silva JLR, Raniero LJ, Lima CSP, Arisawa EAL, Oliveira Cd, et al. Biochemical imaging of normal, adenoma, and colorectal adenocarcinoma tissues by Fourier transform infrared spectroscopy (FTIR) and morphological correlation by histopathological analysis: preliminary results. Research on Biomedical Engineering. 2015;31(1):10-8.

19. Goormaghtigh E. Infrared imaging in histopathology: Is a unified approach possible? Biomedical Spectroscopy and Imaging. 2017;5(4):325-46.

20. Li L, Bi X, Sun H, Liu S, Yu M, Zhang Y, et al. Characterization of ovarian cancer cells and tissues by Fourier transform infrared spectroscopy. J Ovarian Res. 2018;11(1):64-.

21. Durán N, Villela RA Marcato PD, Garcia PV, Ceragioli HJ, Fávaro WJ. *In vivo* evaluation of doxorubicin loaded in r-graphene oxide in bladder cancer model. Nano-2014 Conference, pp. 08.004. Moscow, Russia. 2014; 12(1): 144.

22. Zanin H, Saito E, Ceragioli HJ, Baranauskas V, Corat EJ. Reduced graphene oxide and vertically aligned carbon nanotubes superhydrophilic films for supercapacitors devices. Materials Research Bulletin. 2014;49:487-93.

23. Fávaro WJ, Nunes OS, Seiva FR, Nunes IS, Woolhiser LK, Durán N, et al. Effects of P-MAPA Immunomodulator on Toll-Like Receptors and p53: Potential Therapeutic Strategies for Infectious Diseases and Cancer. Infect Agent Cancer. 2012;7(1):14-.

24. Epstein JI, Amin MB, Reuter VR, Mostofi FK. The World Health Organization/International Society of Urological Pathology Consensus Classification of Urothelial (Transitional Cell) Neoplasms of the Urinary Bladder. The American Journal of Surgical Pathology. 1998;22(12):1435-48.

25. Li Q-B, Xu, Z, Zhang N-W., Zhang L, Wang F, Yang L-M, et al. *In vivo* and *in situ* detection of colorectal cancer using Fourier Transform Infrared Spectroscopy. World Journal of Gastroenterology. 2005; 11(3): 327-30.

26. Naumann D. . Infrared Spectroscopy: New Tool in Medicine; 1998/04/24: SPIE; 1998.

27. Li C, Ebenstein D, Xu C, Chapman J, Saloner D, Rapp J, et al. Biochemical characterization of atherosclerotic plaque constituents using FTIR spectroscopy and histology. Journal of Biomedical Materials Research. 2003;64A(2):197-206.

28. Venkatachalam P, Rao LL, Kumar NK, Jose A, Nazeer SS, Vaidyan VK, et al. Diagnosis of Breast Cancer Based on FT-IR Spectroscopy. AIP Conference Proceedings: AIP; 2008.

29. Kong J, Yu S. Fourier Transform Infrared Spectroscopic Analysis of Protein Secondary Structures. Acta Biochimica et Biophysica Sinica. 2007;39(8):549-59.

30. Farshad H, Niki V, Khosrou A, Ansieh F, Farzaneh BR. Fourier Transform Infrared Spectroscopic comparison of normal and malignant cervical tissue, school of pharmacy. Iranian Journal of Pharmaceutical Research. 2007; 6(2): 107-13.

31. Movasaghi Z, Rehman S, ur Rehman DI. Fourier Transform Infrared (FTIR) Spectroscopy of Biological Tissues. Applied Spectroscopy Reviews. 2008;43(2):134-79.

32. Du JK, Shi J-S, Sun X-J, Wang J-S, Xu Y-Z, Wu J-G, et al. Fourier Transform Infrared Spectroscopy of gallbladder carcinoma cell line. Hepatobiliary. Pancreatic Diseases International. 2009; 8(1):75-8.